https://ntrs.nasa.gov/search.jsp?R=19690004310 2018-07-23T23:51:34+00:00Z

General Disclaimer

One or more of the Following Statements may affect this Document

- This document has been reproduced from the best copy furnished by the organizational source. It is being released in the interest of making available as much information as possible.

- This document may contain data, which exceeds the sheet parameters. It was furnished in this condition by the organizational source and is the best copy available.

- This document may contain tone-on-tone or color graphs, charts and/or pictures, which have been reproduced in black and white.

- This document is paginated as submitted by the original source.

- Portions of this document are not fully legible due to the historical nature of some of the material. However, it is the best reproduction available from the original submission.

Produced by the NASA Center for Aerospace Information (CASI)

N69-13642
(ACCESSION NUMBER) (THRU)
47 1
(PAGES) (CODE)
CR#99913 16
(NASA CR OR TMX OR AD NUMBER) (CATEGORY)
FACILITY FORM 602

Correlations in Light from a Laser at Threshold

R. F. Chang, V. Korenman, C. O. Alley,

and

R. W. Detenbeck

Technical Report No. 883

September 1968

UNIVERSITY OF MARYLAND
DEPARTMENT OF PHYSICS AND ASTRONOMY
COLLEGE PARK, MARYLAND

DEC 1968
RECEIVED
NASA STI FACILITY
INPUT BRANCH

Correlations in Light from a Laser at Threshold *

R. F. Chang, V. Korenman, and C. O. Alley

Department of Physics and Astronomy

University of Maryland, College Park, Maryland

and

R. W. Detenbeck

Department of Physics and Astronomy

University of Maryland, College Park, Maryland

and

Department of Physics

University of Vermont, Burlington, Vermont †

August 29, 1968

* work supported by NASA (grant NGR21-002-022 and NGR46-001-008S2) ARPA (contract SD-101), U. S. Army Research Office (contract DAHC04 67 C 0023, under Project Defender), U. S. Office of Naval Research (contract N000 14-67-A-0239-003), and Air Force Office of Scientific Research (grant AF-735-65) as well as the University of Maryland Computer Science Center under NASA grant NsG-398.

† present address

ABSTRACT

In this study, we measured the temporal correlations in the electromagnetic field radiated by a laser in the threshold region of oscillation, from 1/10 of threshold intensity to ten times threshold intensity. The experimental results are compared with theoretical predictions based on solutions of a Fokker-Planck equation.

We stabilized the intensity of a He-Ne cw gas laser by means of a long-time-constant servo system which controlled the cavity length.

Using a fast photomultiplier as detector, we recorded the photoelectron count distribution within a short counting time (3 microseconds) while the photomultiplier was exposed to the laser light. From the photoelectron count distribution measurement, we calculated second, third, and fourth normalized cumulants of the intensity probability density function of the light field. The normalized cumulant is a measure of "pure" correlations among photons because the contributions from lower order correlations are removed.

The statistics of the photoelectron count distribution shows that the intensity fluctuations at about 1/10 threshold are nearly those of a Gaussian field and continuously approach those of a constant amplitude field as the intensity is raised to about 10 times threshold.

The normalized 2nd, 3rd, and 4th cumulants of the intensity probability density function of the laser light were also measured at 17% and 42% of threshold intensity as counting time was increased from 3 microseconds to 1000 microseconds. The results agree with predictions computed

computed under the assumption that the dependence of the correlation functions on the time variables is the same as for Gaussian light.

CORRELATIONS IN LIGHT FROM A LASER AT THRESHOLD

I. INTRODUCTION

Since the invention of the laser, intensity fluctuation phenomena in laser radiation have been of great interest. It is well known that if the photocount technique is employed in the measurement, the statistics of photoelectron counting reveals information about the statistics of the light intensity fluctuations. The advantage of the photocount technique is the relative simplicity of the measurement of the higher order correlations. In fact, remarkable work has been done with this particular technique in the study of fluctuation phenomena in lasers[1-14].

The first measurements[1-12] showed that well above the threshold of oscillation, a single-mode cw laser produces light of essentially constant amplitude. At the same time, it was demonstrated that such a laser operating far below the threshold generates an electromagnetic field with a nearly Gaussian amplitude distribution. Theories for the single-mode cw laser developed at about this time described the transition from a Gaussian light source to an amplitude-stabilized source[15-24]. These theoretical papers pointed out that the region near threshold is most crucial for a comparison between theoretical predictions and experimental results, but practical difficulties had prevented exploration of this important region in the early experiments. More recently some preliminary experimental results have been presented, by others as well as ourselves[13,14,25,26] which confirm theoretical

predictions based on the solutions of a Fokker-Planck equation for a laser operating near threshold.

This paper presents the detailed results of our study of a single-mode He-Ne laser operating over an intensity range from 1/10 to ten times that at threshold. The results of our photoelectron count measurements are interpreted in terms of the statistics of the light from the laser. We adopt the semi-classical approach and relate the statistics of the photoelectron count distribution to those of the intensity probability density function (IPDF) of the light, and the measure of correlations among photons is represented by the normalized cumulants of the IPDF of the light.

In our experiment, we obtained the normalized cumulants of the laser light IPDF up to fourth order. The results are compared with theoretical predictions based on solutions of a Fokker-Planck equation. The close agreement is remarkable.

II. THEORY OF INTENSITY FLUCTUATIONS

If a phototube is repeatedly exposed to a stationary light field for an interval T, the photoelectron count probability density function can be related to the time-integrated-intensity probability density function of the light field at the photocathode by[27]

$$p(n) = \int_0^\infty \frac{(\alpha U)^n}{n!} e^{-\alpha} \mathcal{P}(U) dU \qquad (1)$$

Here p(n) is the probability of counting precisely n photoelectrons while $\mathcal{P}(U)$ is the probability density function for the time integrated intensity U and α is the quantum efficiency of the photocathode. If we think of the light field in classical terms, then

$$U \equiv \int_t^{t+T} I(t')dt' , \qquad (2)$$

where I(t) is the instantaneous light intensity (integrated over the photocathode volume) while $\mathcal{P}(U)$ is simply the probability of finding the time integrated intensity to be U. In quantum mechanical terms, Eq. (1) still holds except that $\mathcal{P}(U)$ is now defined in terms of its moments as

$$\prod_{i=1}^{n} \int_t^{t+T} dt_i \int d^3r_i \; G^{(n)} (r_1t_1, r_2t_2, \ldots r_nt_n; r_nt_n, \ldots r_2t_2, r_1t_1)$$

$$= \int_0^\infty U^n \mathcal{P}(U) dU \equiv \langle U^n \rangle \qquad (3)$$

where the $G^{(n)}$ are the normally ordered light field correlation functions discussed by Glauber[28].

In general, it is impossible to evaluate Eq. (1) given only the probability density function for the instantaneous light intensity. As is clear from its representation in Eq. (3), $\mathcal{P}(U)$ is a complicated function of the counting interval which depends on the detailed dynamics of the light field fluctuations over the time T. To simplify the discussion and the analysis of the experiment, we restrict ourselves here to the condition that the counting time T is much shorter than the characteristic time for light intensity fluctuations. We may then replace the time integrated intensity in Eq. (2) by T times the instantaneous intensity or, equivalently, in Eq. (3), evaluate $G^{(n)}$ with all times equal and replace the n time integrals by a factor of T^n. We will return below to the more general case of arbitrary T.

Then Eq. (1) can be written as

$$p(n) = \int_0^\infty \frac{I^n}{n!} e^{-I} P(I) dI \tag{4}$$

in intensity units where $\alpha T = 1$ and I, the instantaneous intensity, is a stationary random variable. The function P(I) is the (instantaneous) intensity probability density function, which we call the IPDF.

The intensity probability density function for the light field inside a single mode laser (and thus for the light field at a photocathode illuminated by such a laser) has been evaluated as a steady state solution of a Fokker-Planck equation[12,17,22] to be

$$P(I) = \frac{2}{\pi \langle I_o \rangle} \frac{\exp(-w^2)}{1+\mathrm{erf}(w)} \exp\left[-\frac{I^2}{\pi \langle I_o \rangle^2} + \frac{2wI}{\sqrt{\pi} \langle I_o \rangle} \right] \qquad (5)$$

where

$$\langle I \rangle = \left[\sqrt{\pi}\, w + \frac{\exp(-w^2)}{1+\mathrm{erf}(w)} \right] \langle I_o \rangle, \qquad (6)$$

gives the mean intensity in terms of the mean intensity at threshold, $\langle I_o \rangle$, and a pumping parameter w. When $w > 0$ ($w < 0$) the laser is operating above (below) what is commonly called its "threshold" level. It is this theoretical expression we will be comparing with experiment in the threshold region.

The expected photoelectron count distribution p(n) produced by laser light can be obtained by inserting Eq. (5) into Eq. (4). However, the expression so obtained is not simple[12]. In order to compare experimental results with theoretical predictions, a more convenient meeting point is provided by the IPDF itself and its statistical constants, such as moments. A real experiment with finite uncertainties determines well only a finite number of appropriately chosen statistical constants of the IPDF, and we must try to choose independent statistical constants to maximize the information obtained. We choose to limit our description to constants which are normalized to be independent of the absolute intensity.

Smith and Armstrong have found useful the reduced second moment of intensity H_2,

$$H_2 = \frac{\langle I^2 \rangle}{\langle I \rangle^2} - 1,$$

which is the normalized variance of the IPDF. The appropriate generalization of the variance to a higher moment seems to us to be the normalized cumulant of the IPDF, which subtracts from the i-th moment effects due to correlations of order lower than i (cf. Appendix A).

The most concise definition of the i-th order cumulant K_i of the IPDF is [29]

$$K_i = \frac{d^i}{ds^i} \ln \langle e^{Is} \rangle \Big|_{s=0} . \tag{7}$$

It is shown in Appendix A that in spite of this apparently unphysical formal definition, the closely related normalized cumulants $K_i/K_1^{\,i} = Q_i$ have a significant physical interpretation. The i-th order normalized cumulant is a measure of pure i-photon bunching, excluding the probability of the presence of i photons because of accidental coincidences, or correlations of lower order.

The normalized cumulants are easily evaluated for two particular forms of the IPDF of prime interest. The IPDF of fully polarized light of Gaussian amplitude distribution is[27]

$$P(I) = \langle I \rangle^{-1} \exp\left(-I/\langle I \rangle\right) \tag{8}$$

where $\langle I \rangle$ is the mean intensity. Inserting Eq. (8) into Eq. (7), we

obtain $K_i = (i-1)!\langle I\rangle^i$, or $Q_i = (i-1)!$ The values are appropriate for chaotic or thermal light sources.

For a constant amplitude field such as a laser far above threshold, the IPDF is

$$P(I) = \delta(I - \langle I\rangle). \tag{9}$$

Inserting Eq. (9) into Eq. (7), we obtain $K_1 = \langle I\rangle$, and $K_i = 0$ or $Q_i = 0$ for all $i \geq 2$, which implies that the photons in a constant amplitude field propagate independently and do not bunch.

Similarly, we obtain the cumulants of the theoretical laser IPDF by inserting Eq. (5) into Eq. (7):

$$K_i = \left(\frac{\sqrt{\pi}}{2}\langle I_o\rangle\right)^i r_i(w),$$

or

$$Q_i = r_i(w)/[r_1(w)]^i$$

where[30]

$$r_1(w) = 2w + \frac{2}{\sqrt{\pi}}\frac{\exp(-w^2)}{1+\mathrm{erf}(w)}, \text{ and } r_i(w) = \frac{d}{dw} r_{i-1}(w) .$$

Or explicitly, we have

$$r_2(w) = 2 + 2wr_1(w) - [r_1(w)]^2,$$

$$r_3(w) = 2r_1(w) + 2r_2(w)[w - r_1(w)] ,$$

$$r_4(w) = 2r_2(w)[2 - r_2(w)] + 2r_3(w)[w - r_1(w)] ,$$

etc....

Experimental values for the cumulants of the IPDF are easily extracted from the photocounting data. Thus, from Eq. (4) the factorial moments of p(n)

$$m_{[i]} \equiv \sum_{n=0}^{\infty} \frac{n!}{(n-i)!} p(n)$$

are equal to the corresponding moments of P(I)

$$m_{[i]} = M_i \equiv \langle I^i \rangle \equiv \int_0^{\infty} I^i P(I) dI \tag{10}$$

Factorial cumulants $k_{[i]}$ of p(n) are defined in close analogy to Eq. (7) (cf. Appendix B) and Eq. (10) implies that $k_{[i]} = K_i$ as well. Then our data is analyzed by evaluating the $k_{[i]}$ from the measured distribution and comparing them to theoretically predicted values of the K_i.

III. EXPERIMENTAL SETUP

A block diagram of the experimental arrangement is shown in Fig. 1. The laser used in the experiment was a small single mode He-Ne cw gas laser oscillating at 6328Å. The laser is an early model from the stable-laser development program[31] undertaken by U. Hochuli of the Dept. of Electrical Engineering, University of Maryland.

The 1250 MHz axial mode separation (12 cm cavity) and low gain of the laser, even at the peak of the Doppler-broadened gain curve, assured operation in only one axial mode. The nearly hemispherical configuration of

the cavity and the small capillary gas tube (about 1.5 mm inner diameter) suppressed higher order transverse modes because of the high diffraction loss. The laser gas tube had a discharge length of 5 cm with a Brewster angle window attached to each end of the tube. Each cavity mirror had a transmission of 0.6% at 6328 Å. The laser was DC excited with a typical pumping current of 2.5 mA. The pumping current was regulated electronically within a few parts in 10^5.

A cylindrical ceramic piezoelectric transducer was built into one of the mirror holders to control the cavity length. The piezoelectric transducer formed part of an intensity feedback loop[10] which could be used to set the laser intensity and hold it closely to the chosen value, thus stabilizing the pumping parameter w. The reason for the choice of stabilization by tuning is that we believe that main cause of gain drift in a laser is uncontrolled cavity length changes, particularly those resulting from thermal expansion in the metal of the laser structure. Temperature compensated Invar cavity spacers allowed operation of the laser without thermostatic control in a heavy aluminum box which served as a heat reservoir. The temperature in the box reached a sufficiently stable equilibrium in about eight hours. Furthermore, the output from one end of the laser was monitored by a photomultiplier as shown in Fig. 1. An interference filter peaked at 6328 Å with 20 Å bandwidth was used at the window of the monitor photomultiplier so that only the lasing mode was sensed. The photocurrent was compared with a reference. If the laser was operating at the desired intensity level, the photocurrent was completely cancelled by the reference. A deviation caused

by any small drift in the laser output intensity was amplified and applied in series with the main tuning batteries to the transducer to correct, through the cavity tuning, the intensity drift. The laser was stabilized to less than .5% long-term drift in intensity. The time constant of the amplifier in the feedback circuit was 16 seconds, which was sufficiently long to leave the short-time fluctuations of the laser light unaffected.

The laser was isolated from building vibration by seating the heavy aluminum box on a soft auto inner tube. The combination of the large mass of the box and the small spring constant of the soft inner tube yielded a very low high-frequency transmission cutoff, about two cycles per second. The building vibration, which consisted mainly of higher frequencies, was thus decoupled from the laser.

The laser output from the other end was fed to a photomultiplier which was connected to the counting system. The counting system counted repeatedly the number of single photoelectron pulses occurring in a counting time interval and recorded this number in the memory. After having counted a sufficiently large number of times, we obtained the photoelectron distribution, p(n).

The counting system consisted of an amplifier, a discriminator, a gate generator, a scaler, a control circuit, and a multi-channel (pulse height analyzer) memory, as shown in Fig. 1. The single photoelectron pulses from the counting photomultiplier were amplified and fed to the discriminator, which produced a standard pulse for each photoelectron pulse. The single photoelectron pulses from the counting photomultiplier were amplified and

fed to the discriminator, which produced a standard pulse for each photoelectron pulse. The discriminator was gated by a gate generator. The gate generator was set to have a gate width (which was the counting time of the experiment) of 3 microseconds. The choice of the counting time was made with the restrictions that it be short compared with the relaxation time of the light field intensity but long compared with the dead time of the system. The dead time of the counting system was 39 nanoseconds.

During an open gate period, the standard discriminator output pulses triggered by the photoelectron pulses were counted and the number stored in a scaler with a storage capacity of 128 counts. Before the next gating period was initiated, the information in the scaler was transferred to the memory of a multichannel pulse height analyzer as follows.

At the conclusion of the gating period, a local oscillator in the control circuit was activated. The standard pulse output from the oscillator was used to scale the address scaler of the multichannel memory while it was simultaneously used to fill the partially filled scaler. The oscillator stopped as soon as the scaler was filled to its capacity of 128 counts. Then the control circuit added "one" in the particular address of the multichannel memory to which the address scaler had advanced, and one sampling period was concluded. A signal from the control circuit would initiate the next sampling period.

The sampling cycle was repeated at a rate of about 3 KHz until about 10^5 samples were collected. Then the data in the analyzer memory was read out by a teletype page printer, which punched a paper tape at the same time. The paper tape was then ready for analysis by a digital computer.

IV. SYSTEMATIC CORRECTIONS

In Sec. II, we made the theoretical analysis under the assumptions that the counter was free of dead time effects and the counting time was extremely short (ideally zero). In the actual experiment, however, neither the dead time nor the counting time is zero; therefore, systematic corrections were accordingly applied to the data. Furthermore, a small amount of light from the gas discharge was also present along with the laser light, requiring an extra correction.

1. Dead Time Correction

The counting system has a dead time after recording a photoelectron in which it is insensitive to another event. If a counter has a dead time only for a recorded event but not for one which occurs during the insensitive period following a previous event, then it is called "nonparalyzable". Our counter is such and it has been shown[32] that for such a counter with a dead time τ, the Poisson distribution with mean of x appropriate to constant intensity light must be replaced by the following exact expression

$$p_D(n) = \gamma\ (n-1,\ \beta_{n-1})/(n-1)! - \gamma(n,\ \beta_n)/n! \tag{11}$$

where

$$\gamma(n,\ \beta_n) = \int_0^{\beta_n} v^n e^{-v}\, dv$$

is the incomplete gamma function and $\beta_n = x(1 - n\delta)$ with δ defined as the

ratio of the dead time τ to the counting time T, $\delta = \tau/T$. In order to obtain convenient expressions relating measurements affected by dead time and those free of dead time, Eq. (11) is expanded in powers of δ up to the third, yielding[33]

$$p_D(n) = \frac{x^n e^{-x}}{n!} (1 + A_1\delta + A_2\delta^2/2 + A_3\delta^3/6 + \ldots\ldots) \qquad (12)$$

where

$$A_1 = (x + 1)n - n^2,$$

$$A_2 = -[(x + 1)n - (x^2 + 2x + 3)n^2 + (2x + 3)n^3 - n^4],$$

$$A_3 = (x^2 + 2x + 2)n - (3x^2 + 8x + 9)n^2$$
$$+ (x^3 + 3x^2 + 12x + 16)n^3 - (3x^2 + 9x + 14)n^4 + (3x+6)n^5 - n^6.$$

If we replace the Poisson distribution in the integral of Eq. (4) by Eq. (12), we obtain the relationship between the factorial moment of p(n) with dead time effects, $f_{[i]}$, and the moment of the IPDF, M_i, as

$$f_{[1]} = M_1 - M_2 (\delta - \tfrac{1}{2}\delta^2) + M_3(\delta^2 - \delta^3) - M_4\delta^3 \qquad (13a)$$

$$f_{[2]} = M_2(1-2\delta + \delta^2) - M_3(2\delta - 6\delta^2 + 4\tfrac{2}{3}\delta^3) \qquad (13b)$$
$$+ M_4(3\delta^2 - 12\delta^3) - M_5(4\delta^3)$$

$$f_{[3]} = M_3(1-6\delta + 12\delta^2 - 8\delta^3) - M_4(3\delta - 22\tfrac{1}{2}\delta^2 + 57\delta^3) \qquad (13c)$$
$$+ M_5(6\delta^2 - 54\delta^3) - M_6(10\delta^3),$$

$$f_{[4]} = M_4(1-12\delta + 54\delta^2 - 108\delta^3) - M_5(4\delta - 56\delta^2 + 296\delta^3) \quad (13d)$$

$$+ M_6(10\delta^2 - 160\delta^3) - M_7(20\delta^3),$$

$$f_{[5]} = M_5(1-20\delta + 160\delta^2 -640\delta^3) - M_6(5\delta - 112\tfrac{1}{2}\delta^2 + 1016\tfrac{2}{3}\delta^3 \quad (13e)$$

$$+ M_7(15\delta^2 - 375\delta^3) - M_8(35\delta^3)$$

$$f_{[6]} = M_6(1-30\delta + 375\delta^2 - 2500\delta^3) - M_7(6\delta - 198\delta^2 + 2730\delta^3) \quad (13f)$$

$$+ M_8(21\delta^2 - 756\delta^3) - M_9(56\delta^3),$$

$$f_{[7]} = M_7(1 - 42\delta + 756\delta^2 - 7560\delta^3) - M_8(7\delta-318\tfrac{1}{2}\delta^2 + 6223\delta^3) \quad (13g)$$

$$+ M_9(28\delta^2 - 1372\delta^3) - M_{10}(84\delta^3),$$

and etc..

The practical difficulty attending the use of the corrections is that the corrections needed to obtain M_k from measured $f_{[k]}$ involve higher order moments which themselves require corrections. A consistent method of approximation is obtained by iteration. The uncorrected $f_{[k]}$ is taken as the zeroth order approximation to M_k and designated $M_k(0)$. For i-th order corrections, we retain the terms in δ^j only for all $j \leq i$; and the coefficients of δ^j are given by the (i-j)th order approximation to M_k designated by $M_k(i-j)$ with appropriate values of k. For first order corrections, we obtain

$$M_6(1) = f_{[6]} + \delta[30f_{[6]} + 6M_7(0)],$$

$$M_5(1) = f_{[5]} + \delta[20f_{[5]} + 5M_6(0)],$$

$$M_4(1) = f_{[4]} + \delta[12f_{[4]} + 4M_5(0) \ ,$$

$$M_3(1) = f_{[3]} + \delta[6f_{[3]} + 3M_4(0)] \ ,$$

$$M_2(1) = f_{[2]} + \delta[2f_{[2]} + 2M_3(0)] \ ,$$

$$M_1(1) = f_{[1]} + \delta M_2(0) \quad .$$

For second order corrections, we obtain

$$M_5(2) = f_{[5]} + \delta[20f_{[5]} + 5M_6(1)] + \delta^2[240f_{[5]} - 12\tfrac{1}{2}M_6(0) - 15M_7(0)]$$

$$M_4(2) = f_{[4]} + \delta[12f_{[4]} + 4M_5(1)] + \delta^2[90f_{[4]} - 8M_5(0) - 10M_6(0)]$$

$$M_3(2) = f_{[3]} + \delta[6f_{[3]} + 3M_4(1)] + \delta^2[24f_{[3]} - 4\tfrac{1}{2}M_4(0) - 6M_5(0)]$$

$$M_2(2) = f_{[2]} + \delta[2f_{[2]} + 2M_3(1)] + \delta^2[3f_{[2]} - 2M_3(0) - 3M_4(0)]$$

$$M_1(2) = f_{[1]} + \delta M_2(1) - \delta^2[\tfrac{1}{2}M_2(0) + M_3(0)] \quad .$$

For third order correction, we obtain

$$M_4(3) = f_{[4]} + \delta[12f_{[4]} + 4M_5(2)] + \delta^2[90f_{[4]} - 8M_5(1) - 10M_6(1)]$$
$$+ \delta^3[540f_{[4]} - 16M_5(0) + 40M_6(0) + 20M_7(0)] \tag{14a}$$

$$M_3(3) = f_{[3]} + \delta[6f_{[3]} + 3M_4(2)] + \delta^2[24f_{[3]} - 4\tfrac{1}{2}M_4(1) - 6M_5(1)]$$
$$+ \delta^3[80f_{[3]} - 6M_4(0) + 18M_5(0) + 10M_6(0)] \tag{14b}$$

$$M_2(3) = f_{[2]} + \delta[2f_{[2]} + 2M_3(2)] + \delta^2[3f_{[2]} - 2M_3(1) - 3M_4(1)]$$

$$+ \delta^3[4f_{[2]} - 1\tfrac{1}{3}M_3(0) + 6M_4(0) + 4M_5(0)] \qquad (14c)$$

$$M_1(3) = f_{[1]} + \delta M_2(2) - \delta^2[\tfrac{1}{2}M_2(1) + M_3(1)] + \delta^3[M_3(0) + M_4(0)] \qquad (14d)$$

The accuracy of the third-order expansion in Eq. (13) improves with decreasing δ. The omitted fourth-order terms in $f_{[k]}$ includes $M_j\delta^4$ where $k \leq j \leq k+4$. The convergence of the series is worst for light fields with large fluctuations. In general, $M_k = C_k(M_1)^k$; that is, the k-th moment is proportional to the k-th power of the mean intensity, M_1, times a constant which depends upon the statistical nature of the field fluctuations. For our worst case, the Gaussian field of a laser operating well below threshold, $M_k = k!(M_1)^k$. Thus, the neglected fourth order terms include $(k+4)(k+3)(k+2)(k+1)(k!)(M_1)^{k+4}\delta^4 \times$(constant) whereas the dominant term contains $(k!)(M_1)^k$, and we must require that $k\delta M_1 \ll 1$. Similar considerations apply to the inversion of Eq. (13) to obtain Eq. (14).

The accuracy of the dead time correction was tested as follows. Assuming a dead-time-affected Bose-Einstein photocount distribution[32], which is appropriate to Gaussian light, the moments with dead time effect were calculated. The dead time correction was applied to these moments and then compared with the values of the moments in the absence of the dead time effect. We found that, for a mean of 2 counts, the errors in the corrected first and second moment were negligibly small, and that in the third and fourth moments, the errors were .5% and 2% respectively. Therefore,

in our experiment with $\delta = 0.013$, ($\tau = 39$ nsec, $T = 3$ μsec), we kept M_1 between 1 and 2, by using a few calibrated filters to attenuate the laser light when necessary, to assure the validity of the dead time correction.

2. Counting Time Correction

The necessary condition for our measurements to reflect the statistics of the instantaneous light intensity is that the counting time be much smaller than the coherence time of the intensity fluctuation: $\Gamma T \ll 1$, where Γ is the half width of the intensity fluctuation spectrum. But the precise degree of smallness needed for a given accuracy is not obvious.

Now it is known for a Gaussian light source that the normalized i-th cumulant for a counting interval T is[27]

$$T^i Q_i(T) = Q_i(0) \int_0^T\!\!\int \ldots\ldots \int \gamma(t_1-t_2)\gamma(t_2-t_3)\ldots\ldots\gamma(t_i-t_1)dt_1\ldots dt_i \qquad (15)$$

for $i \geq 2$, where $\gamma(t_i-t_j)$ is the normalized field amplitude correlation function. Assuming the field has a Lorentzian amplitude spectrum, the absolute value of the two-time correlation function decreases exponentially with time separation

$$\left|\gamma(t_i-t_j)\right| = \exp(-\Gamma\left|t_i-t_j\right|/2)$$

where Γ is the half width at half maximum of the intensity power spectrum. Upon substitution of this particular form of the correlation function into

Eq. (15) we obtain[34,35]

$$Q_2(T)/Q_2(0) = 2y^{-1} + 2(e^{-y} - 1)y^{-2} , \tag{16a}$$

$$Q_3(T)/Q_3(0) = 6(e^{-y} + 1)y^{-2} + 12(e^{-y} - 1)y^{-3} , \tag{16b}$$

$$Q_4(T)/Q_4(0) = 8e^{-y}y^{-2} + 20(2e^{-y} + 1)y^{-3} + 2(e^{-2y} + 28e^{-y} - 29)y^{-4} , \tag{16c}$$

where $y = \Gamma T$.

A close examination of Eq. (16) shows that the normalized cumulants deviate from their zero-counting-time limits by 3%, 5%, and 7%, respectively, for the second, third, and forth order, even when y is as small as 0.1.

A preliminary measurement of the spectrum of the laser light showed that the half width Γ was about 6×10^4 sec^{-1} when the laser was operating at about 1/6 of threshold intensity. Then ΓT was about .2 at that point with our counting time of 3 microseconds. In that region, the laser behaves roughly as a Gaussian light source, the computation above is appropriate, and we find that the deviations of the normalized cumulants from their zero-counting-time limits are not negligible.

In order to find appropriate counting time corrections to the statistics of the laser light, we determined the time dependence of the normalized second, third and fourth cumulants for counting times from

3 to 1000 microseconds for a laser operating slightly below threshold where Q_3 and Q_4 are sensibly different from zero. The results were then compared with a time dependence computed under the assumptions that the dependence of the correlation functions on their time variables is that of Gaussian light and the spectrum of the correlation functions is Lorentzian [25]. The results so computed have the same form as Eq. (16)[36]. The validity of Eq. (16a) depends only on the Lorentzian assumption, but the relevance of Eqs. (16b) and (16c) depends upon the dynamical correlations in the laser light.

Our experimental results, which are presented in the next section, show a good agreement with Eq. (16). Therefore, the counting time correction can be applied to the data by using Eq. (16) for the laser operating in the region below threshold. At higher intensities, where the simple assumptions may no longer be applicable, the normalized cumulants approach zero and the counting time correction is comparable to or even less than the systematic error. Therefore, the counting time correction can be ignored.

All bandwidths of the spectra of the laser light were not measured individually for purposes of the counting time corrections. Instead, we measured the width of the spectrum at 17% of threshold intensity where $\Gamma \approx 81.4 \times 10^3$ sec^{-1} and then extrapolated this to other intensities by fitting the data to the quasilinear approximation[21]. We obtained for T = 3 microseconds

$$\Gamma T = 0.041 \left(0.636 \frac{\langle I \rangle}{\langle I_o \rangle} + \frac{\langle I_o \rangle}{\langle I \rangle}\right) . \tag{17}$$

This approximation is quite accurate, with errors less than 3%, for a laser operating below threshold where the counting time correction is the most significant. The error rises to the maximum of 30% at about three times the threshold where the counting time corrections are already insignificant. Therefore, we believe that Eq. (17) is adequate for our purpose.

3. Background Correction

Although an interference filter as well as a geometrical stop was used in front of the counting photomultiplier to reduce the amount of discharge light reaching the photocathode, there was still a small yet not negligible amount of discharge light present. The background electron count was then due mainly to the discharge light, whose intensity was about 5% of the mean intensity of the laser light at threshold and a small amount of dark current which constituted about 1 to 2% of the total counts. In order to obtain the statistics of laser light alone, the background should be removed. Thus, the statistics of the background were first measured and studied.

We measured the photoelectron count distribution due to the total background and found that it followed a Poisson distribution for a counting time of 3 microseconds. A spectral measurement of the background showed a flat spectrum, indicating the broadband nature of the background component.

The total IPDF sensed by the photomultiplier is the convolution of the individual IPDF of the laser light with the equivalent IPDF of

the independent broadband background. It can be shown that any cumulant of the total IPDF is the simple sum of the corresponding cumulant of the laser light and that of the background[37]. Therefore, in the experiment, the cumulants of the background were all measured and then subtracted from the total cumulants to produce the cumulants of the laser light IPDF.

V. RESULTS AND DISCUSSION

1. Statistics of Laser Light at Threshold

The normalized second, third and fourth cumulants of the IPDF of light produced by the laser operating in the region from 1/10 to ten times mean threshold intensity were measured. The counting time was 3 microseconds. All systematic corrections were applied to the data as described above.

The results are plotted as functions of mean intensity in units of mean threshold intensity in Fig. 2. The value of mean threshold intensity $\langle I_o \rangle$ for the laser was obtained from the value of Q_2 in order to place the curves on the abscissa. The laser is at the threshold when $Q_2 = 0.5708$ as described by the theory. The experimental data are shown as dots while the theoretical predictions are the smooth curves. Standard deviations are shown as bars when they are larger than the dot size.

The agreement between the theory and the experiment is very good. As shown in the figures, the laser can be described as a narrow band Gaussian source when it is operating well below threshold ($\langle I \rangle / \langle I_o \rangle \approx 0.1$) as indicated by values of Q_i being nearly $(i-1)!$. The gradual transition of a laser field from a field of Gaussian amplitude distribution to a coherent field when it is brought from well below threshold to well above threshold is properly described by these normalized cumulants which are the measures of bunching effects amoung photons. A gradual decrease in the bunching effects is exhibited by the laser when its mean output power is

increased from 1/10 to 10 times mean threshold intensity. Furthermore, the higher order bunching effects diminish more rapidly than the lower ones. As shown in the figures, Q_4 is almost zero as soon as the laser reaches the threshold, Q_3 does not vanish until the laser reaches about three times threshold, while Q_2 stays non-vanishing until more than ten times threshold. The dramatic transition of a laser field from Gaussian to coherent state is thus demonstrated by our results, which also offer striking confirmation of the theoretical analyses.

2. Counting Time Dependence of the Laser Light Statistics

To facilitate corrections for finite counting times, the normalized second, third, and fourth cumulants of the IPDF of light from the laser operating slightly below threshold were measured as functions of the counting time T. The counting time was varied from 3 to 1000 microseconds. Dead time and background corrections were applied to the data as described in section IV. Then a least squares fit was made of the data $Q_2(T)$ to (the logarithm of) Eq. (16a) using $Q_2(0)$ and Γ as parameters. The same value of Γ was used for $Q_3(T)$ and $Q_4(T)$, adjusting $Q_3(0)$ and $Q_4(0)$ for the best fit. Data for $Q_i(T)/Q_i(0)$, for i = 2, 3, and 4, along with Eq. (16) (shown as smooth curves) are shown in Fig. 3.

Data were obtained at two intensity levels of laser operation. Comparing the best fit values of $Q_2(0)$ with theory, we found that these intensity levels were at 17% and 42% of mean threshold intensity (indicated by open and solid circles, respectively, in the figure). The ratio of the

measured linewidths at these two intensities is $\Gamma(.17)/\Gamma(.42) = 2.20$, in good agreement with the theoretical prediction of 2.19. The values of $Q_3(0)$ and $Q_4(0)$ are also in good agreement (a few percent) with theoretical predictions for these intensities.

The good fit of our experimental results, shown in Fig. 3, seems to imply that in the region under study where the static intensity correlations are already quite different from their Gaussian limits, the dynamic correlations can still be described by the simple one-decay-time approximation appropriate to Gaussian light. At higher intensities, closer to and above the threshold, we expect deviations from this simple result.

Furthermore, this demonstrates that measurements of this kind are quite suitable for measuring spectral linewidths on the order of a megahertz or less. This technique has also recently been used, by Jakeman et al, to measure the spectral half-width of scattered light from particles undergoing Browian motion[38] and is applicable to a variety of systems.

VI CONCLUSION

The measurements presented here have shown that the intensity fluctuations of a laser operating in the threshold region are well described by the theoretical treatments of references 17 - 24. A recent measurement by Arecchi et al[13] of the reduced second order factorial moment, which is the normalized second cumulant of the IPDF, also agrees with these treatments.

As the result of our study, we have not only learned about the correlations in the field radiated by a laser but also established a general approach to measuring the correlations in an electromagnetic field of an arbitrary kind. Further applications of these techniques are under study.

ACKNOWLEDGMENT

The authors are pleased to acknowledge their large debt to Professor Urs Hochuli for the design and construction of the ultra-stable laser used in this investigation and to express their gratitude for his willingness to make it available.

APPENDIX A: MOMENTS, CUMULANTS, AND PHOTON BUNCHING

For either the zero counting time or zero intensity limit, Eq. (4) is exact. In an actual experiment, measurements with nonzero counting time can be extrapolated to the zero counting time limit. In this limit, the i-th moment of the intensity $\langle I^i \rangle$, is a measure of the probability of observing i photons bunching or arriving simultaneously. This is obvious when we consider $\langle I^i \rangle$ in the quantum mechanical sense as $\langle E^{(+)i} E^{(-)i} \rangle$ where $E^{(+)}$ and $E^{(-)}$ are the creation and annihilation operators. If the photons are uncorrelated then the probability of observing i-photon bunching $\langle I^i \rangle$ is equal to the i-th power of probability of observing one photon. This can be expressed as $\langle I^i \rangle = \langle I \rangle^i$, indicating bunching of an accidental kind. A field with only accidental bunching is represented quantum mechanically by a coherent state[28], or classically by a constant intensity. In order to obtain a measure of correlated bunching in excess of the accidental kind, we have to remove all the contributions to the higher order bunching resulting from accidental bunching of lower order. For two-fold correlation we can express the overall bunching by the sum of true bunching and accidental bunching as $\langle I^2 \rangle = K_1^2 + C_2$ where $K_1 \equiv \langle I \rangle$ and C_2 is the two-fold true bunching. For three-fold correlation, we have not only accidental bunching of three single photons but also the accidental bunching of one correlated pair and a single besides the three-fold true bunching C_3. Since the bunching

of a pair and a single can occur in three different ways, the overall three-fold bunching can be expressed by

$$\langle I^3 \rangle = K_1^3 + 3K_1C_2 + C_3 \quad .$$

Applying the same procedure to the four-fold bunching and we obtain

$$\langle I^4 \rangle = K_1^4 + 4K_1C_3 + 6K_1^2C_2 + 3C_2^2 + C_4 \quad .$$

Similarly, any given r-fold bunching $\langle I^r \rangle$ can be expressed in terms of all possible combinations of lower order bunching with a residual term C_r. Reviewing the general formula for moments M_r expanded in terms of cumulants (cf, ref. 29 p. 68),

$$M_r = r! \sum_{i=1}^{r} \sum \prod_{j=1}^{i} [K_{p_j}/(p_j!)]^{\pi_j}/(\pi_j!)$$

where the second summation extends over all non-negative integral value of π_j and p_j such that

$$\sum_{j=1}^{i} p_j\pi_j = r,$$

we find that the expansion of $\langle I^i \rangle$ into true correlations is the same as the expansion of M_r into cumulants. Therefore, we can identify the measures of true bunching, C_i, as the cumulants K_i, and we conclude that the cumulants measure the true bunching of photons.

The values of the cumulant depend on the mean of the distirbution. For a population of the same statistical nature, the higher the mean the larger will the cumulants be. In order to obtain a set of descriptive constants to characterize the statistical nature of the population, we introduce normalized cumulants Q_i, defined as K_i/K_1^i . Notice that the normalized second cumulant Q_2 is the same as the reduced second moment H_2 introduced by Smith and Armstrong.

APPENDIX B: INTERRELATIONSHIPS AMOUNG STATISTICAL CONSTANTS

The factorial moments and factorial cumulants are defined only for a discrete random variable whereas the moments and the cumulants are defined for either a discrete or a continuous random variable. These statistical constants are more conveniently defined by the generating functions. The factorial moment generating function, f(s), of p(n) is defined as[29]

$$f(s) \equiv \sum_{n=0}^{\infty} (1+s)^n \, p(n) \equiv \sum_{i=0}^{\infty} m_{[i]} \frac{s^i}{i!} \quad , \tag{18}$$

and the factorial cumulant generating function, c(s), of p(n) is defined as [29]

$$c(s) \equiv \ln f(s) \equiv \sum_{i=1}^{\infty} k_{[i]} \frac{s^i}{i!} \quad . \tag{19}$$

The moment generating function, M(s), of P(I) is defined as [29]

$$M(s) \equiv \langle e^{Is} \rangle \equiv \sum_{i=0}^{\infty} M_i \frac{s^i}{i!} \quad , \tag{20}$$

and the cumulant generating function, K(s), of I(I) is defined as [29]

$$K(s) \equiv \ln M(s) \equiv \sum_{i=1}^{\infty} K_i \frac{s^i}{i!} \quad . \tag{21}$$

It has been shown that $m_{[i]} = M_i$ in Sec. II, then it follows, comparing Eq. (18) and Eq. (20), that

$$f(s) = M(s).$$

Thus, comparing Eq. (19) and Eq. (21), we have

$$k_{[i]} = K_i \quad .$$

The relationship between $K_{[i]}$ and $m_{[i]}$ can be obtained by expanding the logarithm of Eq. (18) in Eq. (19) and comparing the coefficients of s^i. Explicitly we have[29]

$$k_{[1]} = m_{[1]} \quad ,$$

$$k_{[2]} = m_{[2]} - m^2_{[1]} \quad ,$$

$$k_{[3]} = m_{[3]} - 3m_{[2]}m_{[1]} + 2m^3_{[1]} \quad ,$$

$$k_{[4]} = m_{[4]} - 4m_{[3]}\, m_{[1]} - 3m^2_{[2]} + 12m_{[2]}m^2_{[1]} - 6m^4_{[1]} \quad ,$$

etc..

Footnotes

1. R. L. Bailey and J. H. Sanders, Phys. Letters 10, 295 (1965)
2. J. A. Armstrong and A. W. Smith, Phys. Rev. Letters 14, 68 (1965)
3. J. A. Armstrong and A. W. Smith, Phys. Rev. 140, A155 (1965)
4. F. T. Arecchi, Phys. Rev. Letters 15, 912 (1965)
5. C. Freed and H. A. Haus, Phys. Rev. Letters 15, 943 (1965)
6. C. Freed and H. A. Haus, J. QE 2, 190 (1966)
7. J. A. Armstrong and A. W. Smith, Phys. Letters 19, 650 (1966)
8. C. Freed and H. A. Haus, Phys. Rev. 141, 287 (1966)
9. F. T. Arecchi, E. Gatti, and A. Sona, Phys. Letters 20, 27 (1966)
10. F. T. Arecchi, A. Berne, A. Sona, and P. Bulamacchi, J. QE 2, 341 (1966)
11. F. T. Arecchi, A. Berne, and P. Bulamacchi, Phys. Rev. Letters 16 32 (1966)
12. A. W. Smith and J. A. Armstrong, Phys. Rev. Letters 16, 853 (1966)
13. F. T. Arecchi, G. S. Rodari, and A. Sona, Phys. Letters 25A, 59 (1967)
14. R. F. Chang, R. W. Detenbeck, V. Korenman, C. O. Alley and U. Hochuli, Phys. Letters 25A, 272 (1967)
15. M. Scully and W. E. Lamb, Phys. Rev. Letters 16, 853 (1966)
16. J. A. Fleck, Phys. Rev. 149, 309 and 322 (1966)
17. H. Risken, Z. Physik 186, 85 (1965)
18. H. Risken, Z. Physik 191, 302 (1966)
19. H. Risken and H. D. Vollmer, Z. Physik 201, 323 (1967)
20. H. Risken and H. D. Vollmer, Z. Physik 204, 240 (1967)
21. M. Lax, Bull. Am. Phys. Soc. 11, 111 (1966)

22. R. D. Hempstead and M. Lax, Phys. Rev. 161, 350 (1967)

23. M. Lax, J. QE 3, 37 (1967)

24. M. Lax, W. H. Louisell, J. QE 3, 47 (1967)

25. F. T. Arecchi, M. Giglio, and A. Sona, Phys. Letters 25A 341 (1967); see also F. Davidson and L. Mandel, Phys. Letters 25A, 700 (1967)

26. H. Gamo, R. E. Grace and T. J. Walter, International Quantum Electronics Conference, May 1968

27. L. Mandel, Progress in Optics, edited by E. Wolf (North-Holland Publishing Company, Amsterdam, 1963) Vol. II, p. 181.

28. R. J. Glauber, Phys. Rev. 130, 2529 (1963); and 131, 2766 (1963); see also Quantum Optics and Electronics, edited by DeWitt, Blandin, Cohen - Tannoudji (Gordon and Breach, New York, 1965) pp. 63 ff.

29. M. G. Kendall and A. Stuart, The Advanced Theory of Statistics, (Hafner Publishing Company, New York, 1963), Vol. I.

30. We thank Dr. H. Risken for pointing out to us this simple relation among cumulants.

31. U. Hochui and P. Haldemann, Rev. Sci. Instr. 36, 1493 (1965)

32. G. Bedard, Proc. Phys. Soc. (London) 90, 131 (1967)

33. F. A. Johnson, R. Jones, T. P. McLean and E. R. Pike have obtained the second order expansion, Phys. Rev. Letters 16, 589 (1966)

34. G. Bedard, Phys. Rev. 151, 1038 (1966)

35. E. Jakeman and E. R. Pike, J. Phys. A, 1, 128 (1968)

36. R. F. Chang, V. Korenman and R. W. Detenbeck, Phys. Letters 26A, 417 (1968)

37. H. Cramer, Mathematical Methods of Statistics, (Princeton University Press, Princeton, 1966)

38. E. Jakeman, C. J. Oliver, and E. R. Pike, Preprint "A Measurement of Optical Line Width by Photon-Counting Statistics"

Figure Captions

Fig. 1 Block diagram of the experimental setup.

Fig. 2 Normalized (a) second, (b) third, and (c) fourth cumulant of laser light IPDF plotted as functions of the normalized intensity $\langle I\rangle/\langle I_o\rangle$ in the threshold region. The curves are the theoretical predictions whereas the dots are the experimental data. The indicated error bars (shown when larger than dot size) are standard deviations.

Fig. 3 Normalized (a) second, (b) third, and (c) fourth cumulant of the time integrated IPDF of laser light just below threshold plotted as functions of the counting time. The open circles and the solid circles are the experimental values of laser light operating at 17% and 42%, respectively, of the threshold intensity. The curves are the plots of equation (16). Standard deviations are shown as bars when they are larger than the dot size.

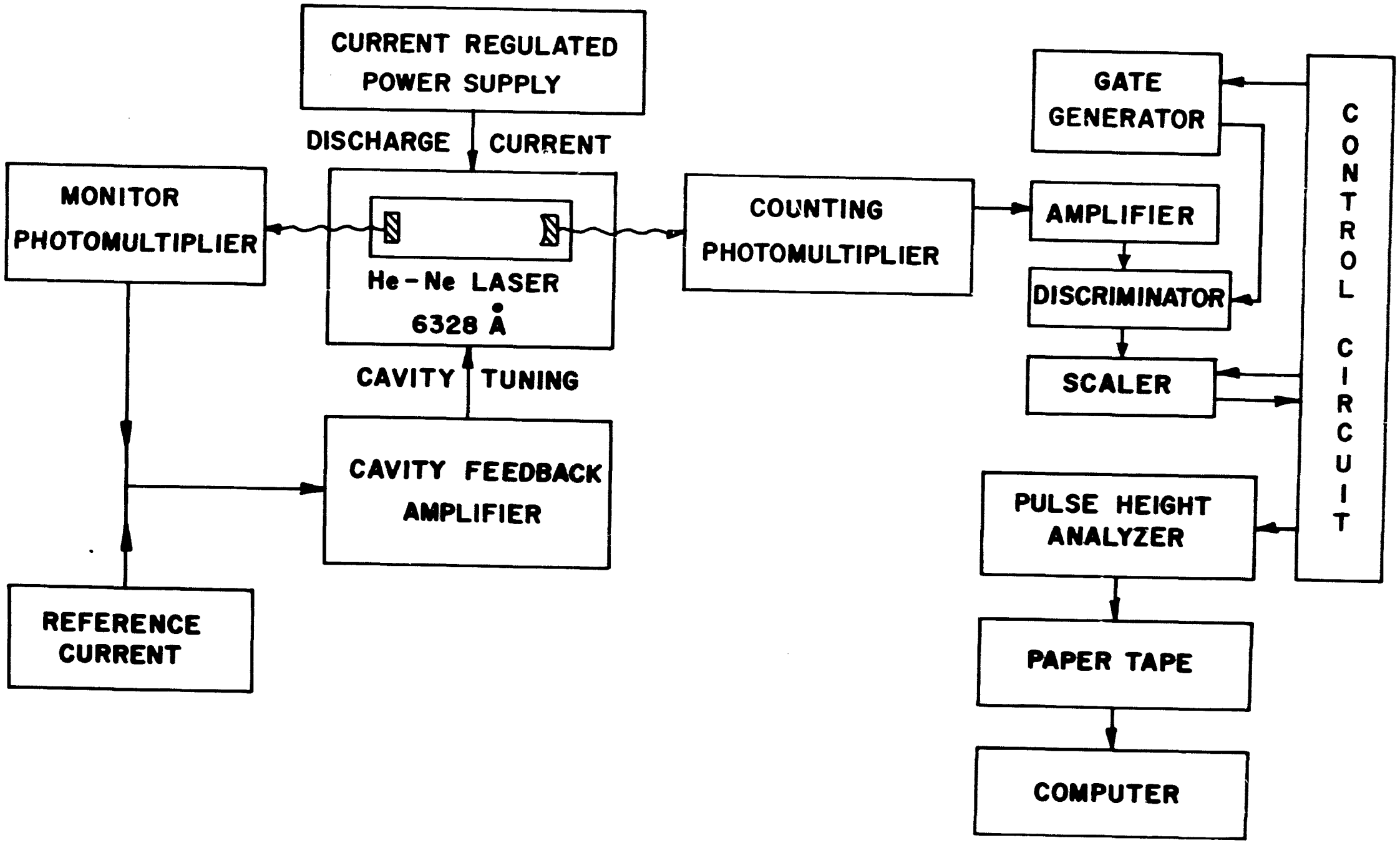
CURRENT REGULATED POWER SUPPLY
DISCHARGE CURRENT
MONITOR PHOTOMULTIPLIER
He-Ne LASER
6328 Å
COUNTING PHOTOMULTIPLIER
GATE GENERATOR
AMPLIFIER
DISCRIMINATOR
SCALER
CONTROL CIRCUIT
CAVITY TUNING
CAVITY FEEDBACK AMPLIFIER
PULSE HEIGHT ANALYZER
PAPER TAPE
COMPUTER
REFERENCE CURRENT

Fig. 1

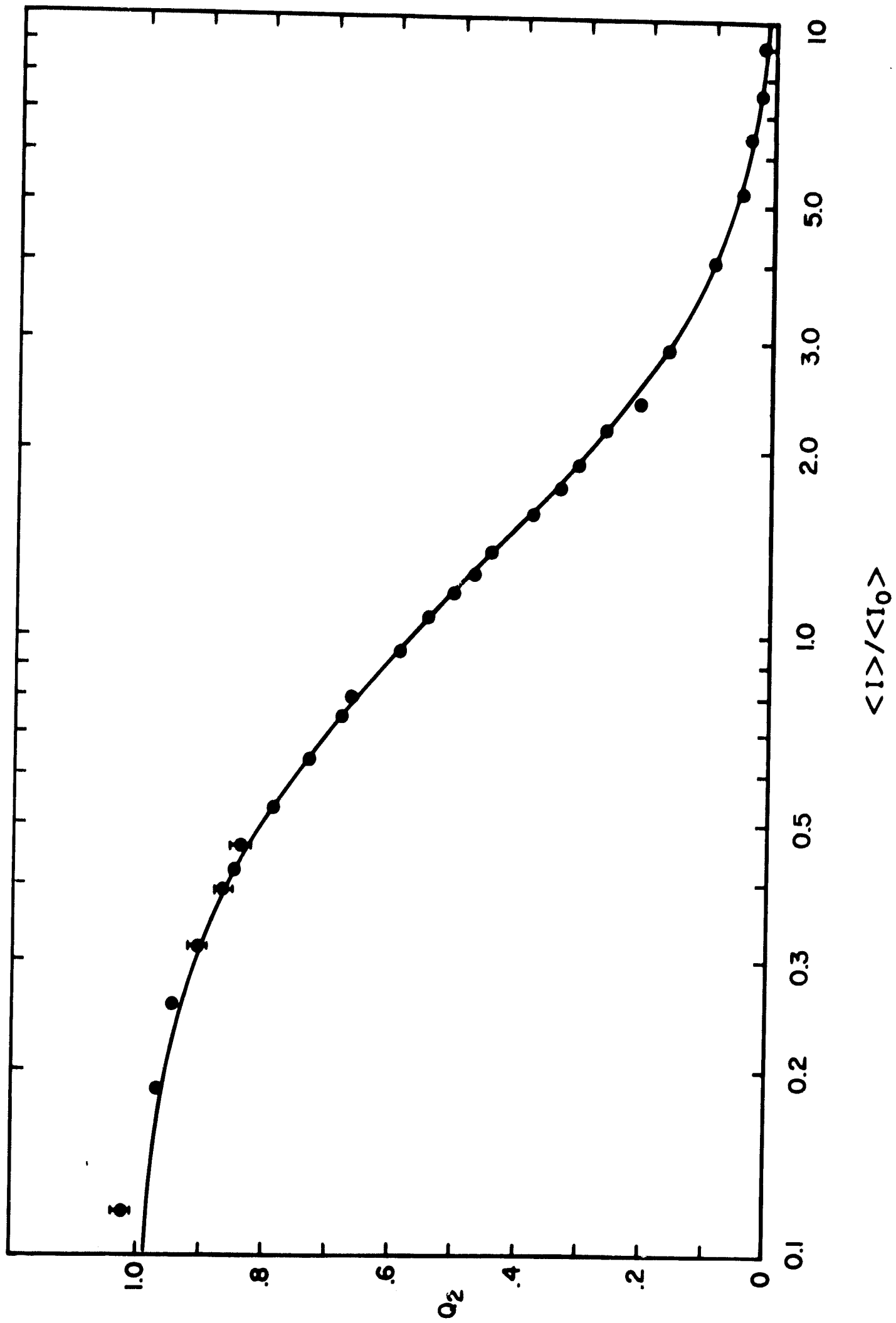
1.0
.8
.6
.4
.2
0
Q^2
0.1
0.2
0.3
0.5
1.0
2.0
3.0
5.0
10
$\langle I \rangle / \langle I_0 \rangle$

Fig. 2a

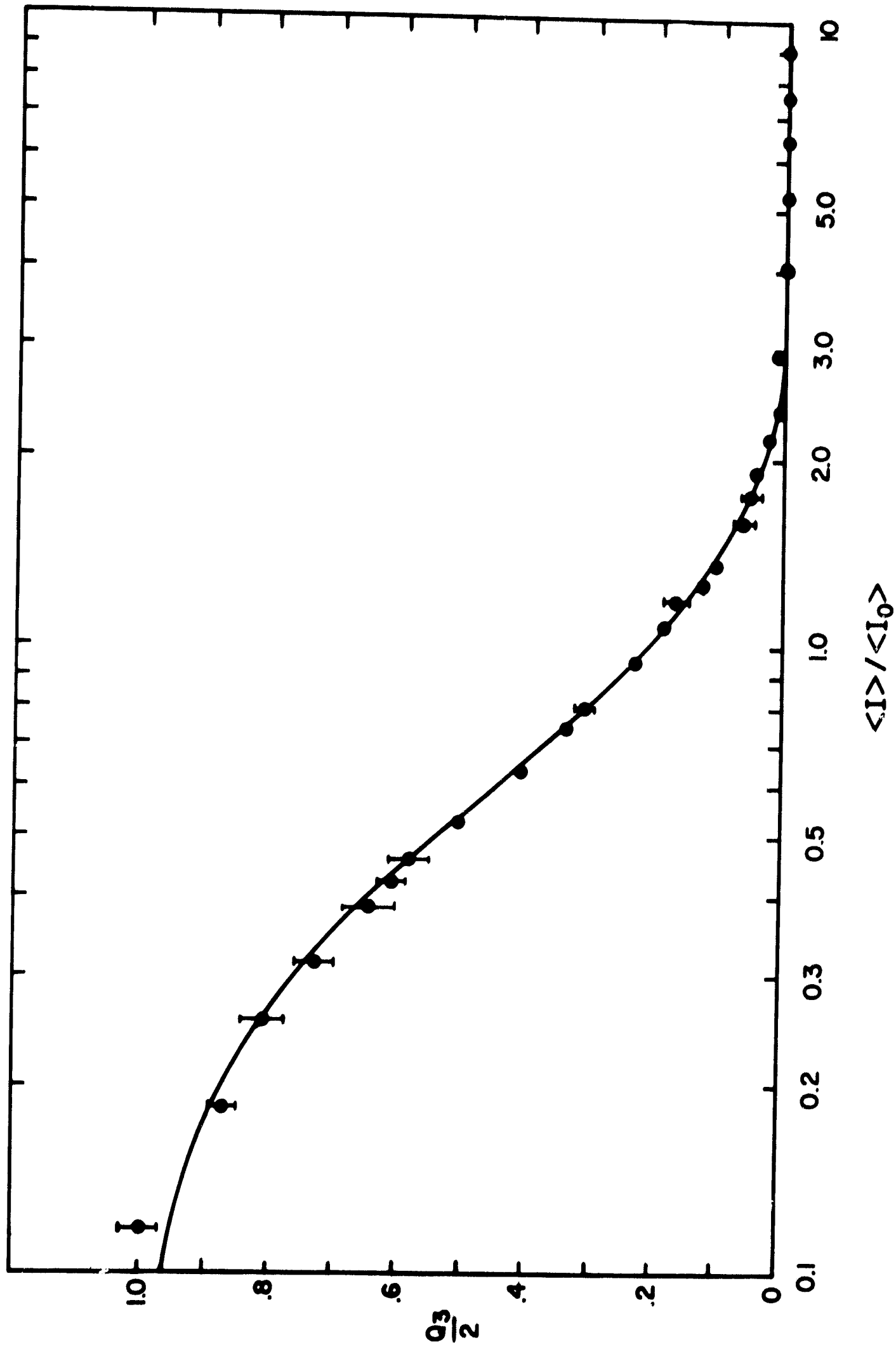
1.0
.8
.6
.4
.2
0
$Q^3/2$
0.1
0.2
0.3
0.5
1.0
2.0
3.0
5.0
10
$\langle I \rangle / \langle I_0 \rangle$

Fig. 2b

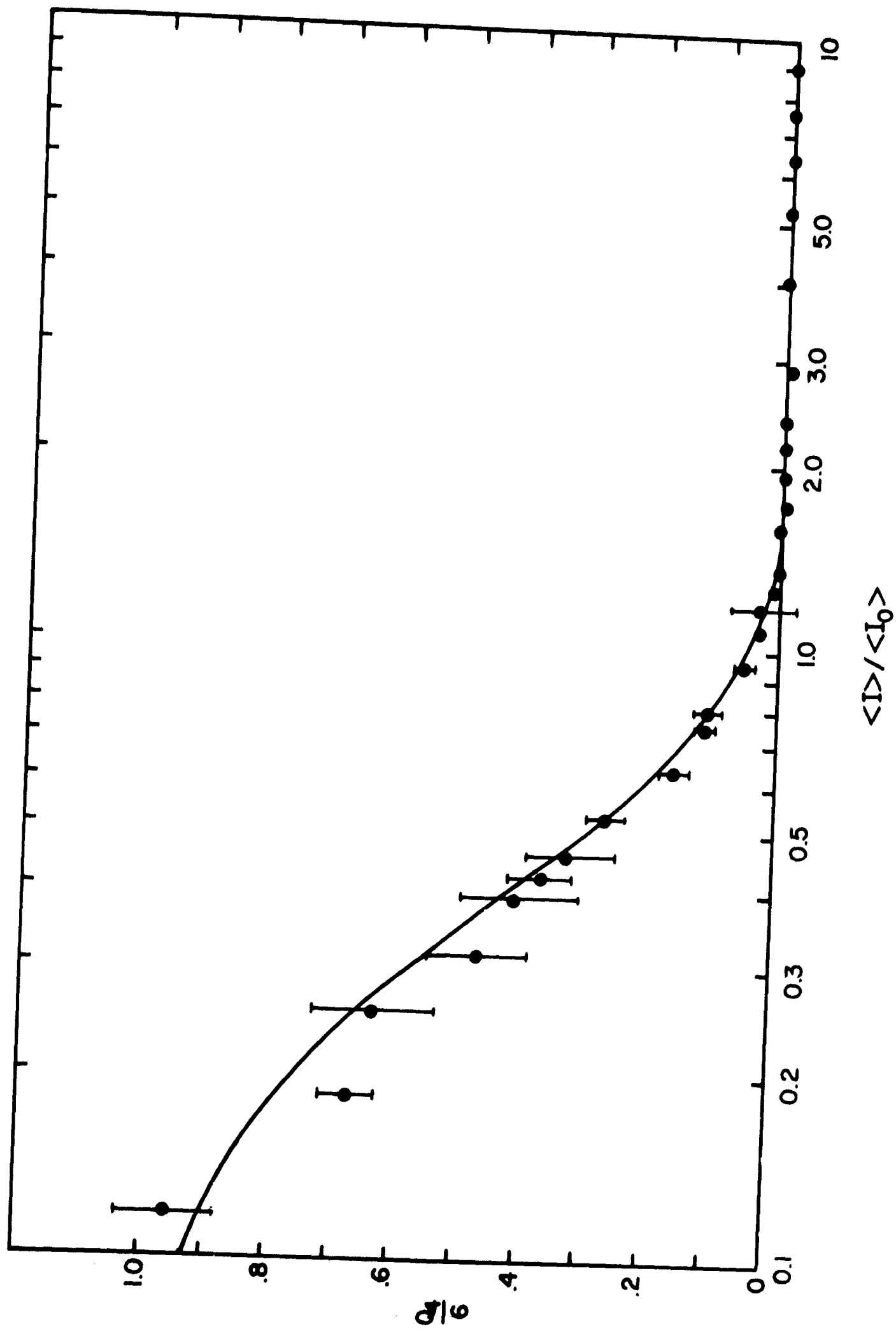
1.0
.8
.6
.4
.2
0
0.1
0.2
0.3
0.5
1.0
2.0
3.0
5.0
10
$\langle I \rangle / \langle I_0 \rangle$

Fig. 2c

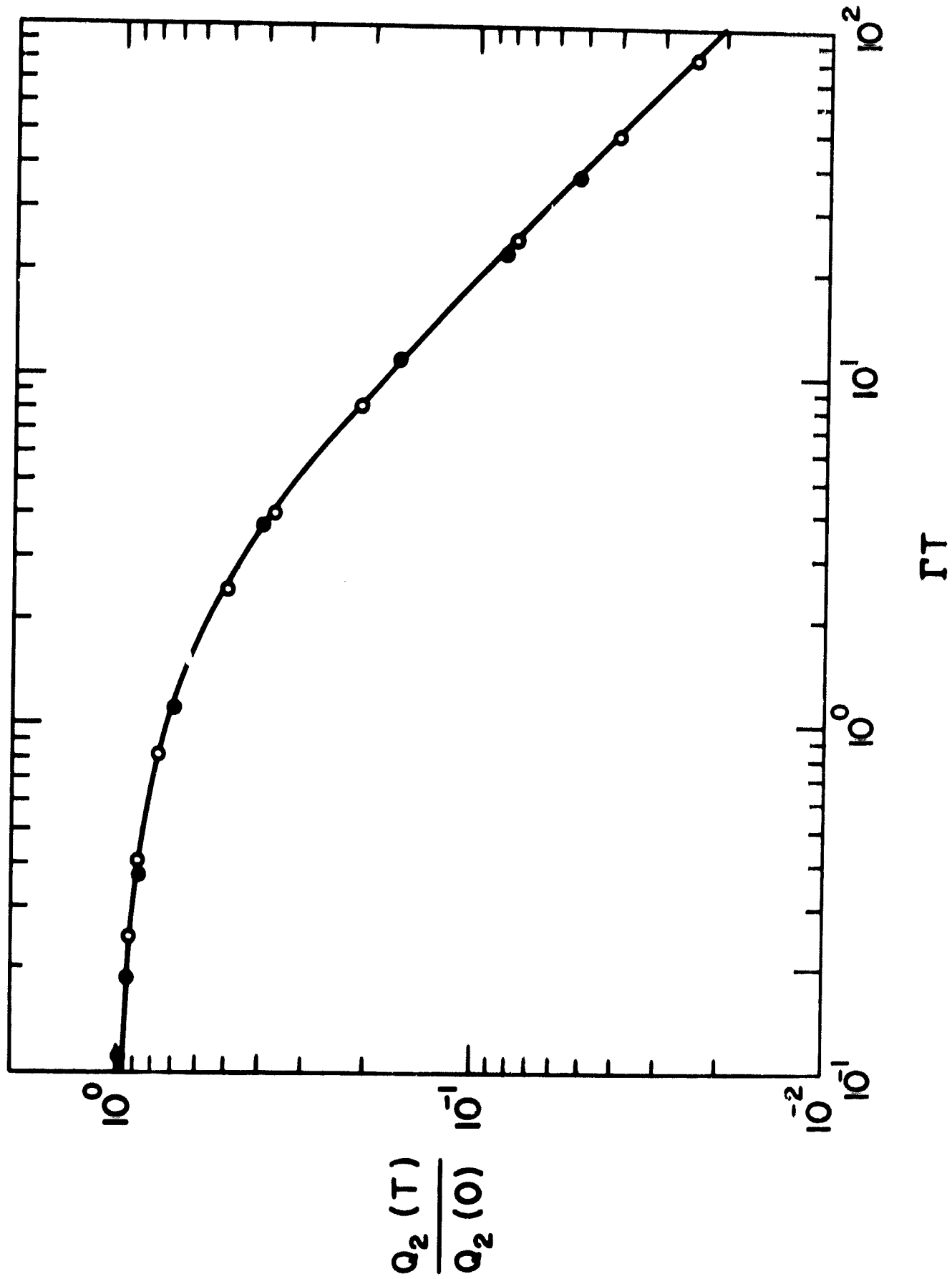

Fig. 3 a

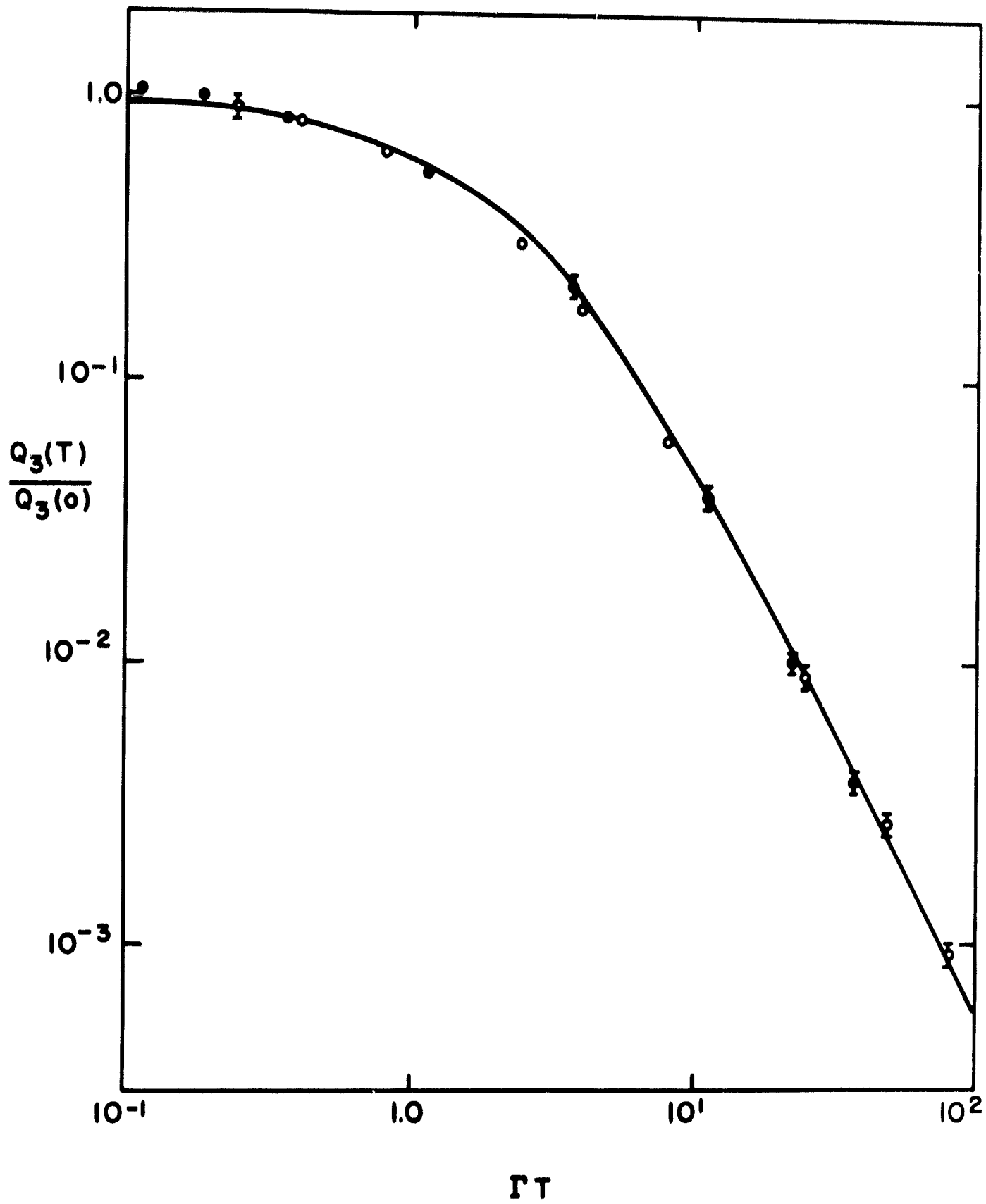

Fig. 3b

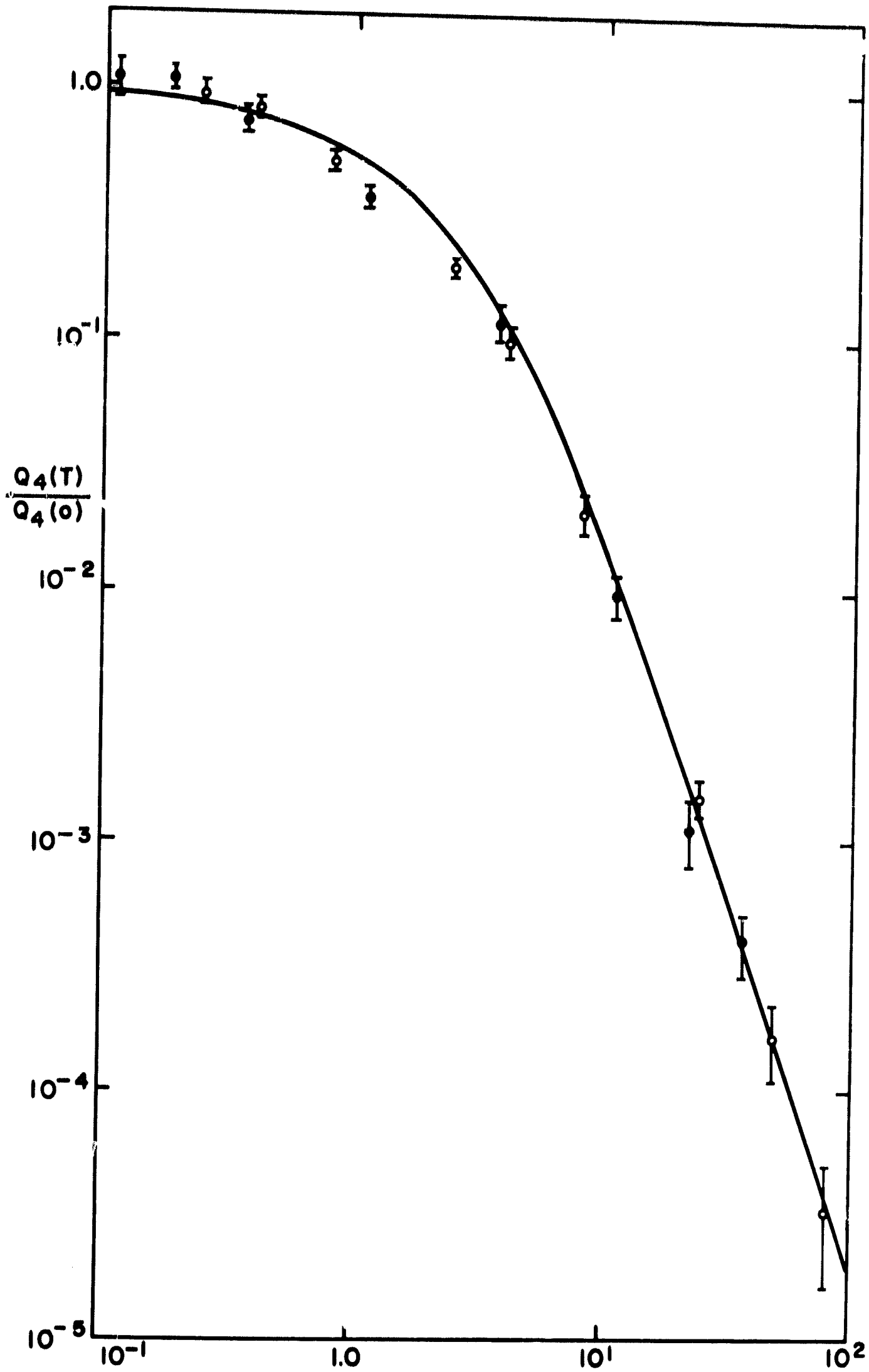

Fig. 3c